

Increased Nonstationarity of Stormflow Threshold Behaviors in a Forested Watershed Due to Abrupt Earthquake Disturbance

Guotao Zhang¹, Peng Cui^{1,2}, Carlo Gualtieri³, Nazir Ahmed Bazai², Xueqin Zhang¹, Zhengtao Zhang⁴

¹ Key Laboratory of Land Surface Pattern and Simulation, Institute of Geographic Sciences and Natural Resources Research, Chinese Academy of Sciences, Beijing 100101, China

² China-Pakistan Joint Research Center on Earth Sciences, Chinese Academy of Sciences and Higher Education Commission, Islamabad 45320, Pakistan

³ University of Napoli Federico II, 80125 Napoli, Italy

⁴ The Key Laboratory of Environmental Change and Natural Disaster, Ministry of Education, Beijing Normal University, Beijing 100875, China

Correspondence to: Peng Cui (pengcui@imde.ac.cn)

Abstract. Extreme earthquake disturbances to local and regional landscape vegetation could ~~swiftly~~rapidly impair ~~original~~former hydrologic functioning, significantly increasing the challenge of predicting threshold behaviors of rainfall-runoff processes as well as the hydrologic system's complexity over time ~~nonstationarity and complexity in threshold behaviors of rainfall runoff processes~~. It is still unclear how alternating catchment hydrologic behaviors under an ongoing large earthquake disruption are mediated by long-term interactions of landslides and vegetation evolutions. In a famous Wenchuan earthquake-affected watershed, in China, the presence and form of the nonlinear hydrologic behavior is examined as having two thresholds with intervening linear segments ~~three linear stormflow threshold behaviors are~~ examined, and both thresholds are identified as a diagnostic tool to characterize variations in hydrologic emergent patterns pre- and post-earthquake. It was revealed that a lower rising threshold (T_r) value (210.48) ~~observed~~ in post-earthquake local landslide regions exhibited faster a stormflow responses response faster than that in undisturbed forest and grass-shrub regions, possibly easily triggering huge flash flood disasters. Additionally, an integrated response metric pair (integrated watershed average generation threshold T_{e-JWA} and rising threshold T_{r-JWA}) with areas of disparate land use, ecology, and physiography was proposed and efficiently applied to identify catchment hydrologic emergent behaviors. The interannual variations of two hydrologic thresholds pre- and post-earthquake were assessed to detect the temporal nonstationarity in hydrologic extremes and nonlinear runoff response. The year 2011 was a turning time in the unsteady recovery process, as post-earthquake landslides evolutions reached a state of extreme heterogeneity in space. At that time, the T_{r-JWA} value decreased by ~ 9 mm compared to the pre-earthquake level. This is closely related to the fast expansion of landslides leading to a larger extension of variable source area from channel to neighboring hillslopes and faster subsurface stormflow contributing to flash floods. Finally, we present a conceptual model interpreting how the short- and long-term interactions of earthquake-induced landslides and vegetation affect flood hydrographs at event timescale that generated an increased nonstationary hydrologic behavior. This study expands our current knowledge about threshold-based hydrological and nonstationary stormflow behaviors in response to abrupt earthquake disturbance for the prediction of future flood regimes.

设置了格式: 字体: Times New Roman

设置了格式: 字体: (默认) Times New Roman, (中文) Times New Roman

设置了格式: 字体: 非倾斜

1 Introduction

35 Appropriately understanding and measuring the hydrological processes from local runoff generation mechanisms to larger watershed scales is difficult due to their complexity and nonlinearity (Farrick and Branfireun, 2014; Ross et al., 2021; Scaife et al., 2020). Previous researchers made some efforts to identify the integrated, physically-based hydrologic processes of [the rainfall-runoff relationship](#) to predict and simulate catchment runoff behavior under different conditions. However, it cannot be generally applied due to uncertainties about water cycle processes, climate inputs, and complex physiographic boundary conditions. [The observed hillslope- or catchment-scale threshold runoff response](#) (Zehe and Sivapalan, 2009; Fu et al., 2013a; Ross et al., 2021; Wang et al., 2022) [shows](#) a hydrologic emergent [pattern, which could be used to identify key hydrologic signatures across different spatiotemporal scales](#) (Ali et al., 2013). [The hydrologic threshold is the critical point in time or space at which abrupt change in stormflow response occurs](#) (Ali et al., 2013). [Below the hydrologic threshold, a small stormflow enters the adjacent channel, but significantly higher runoff magnitudes generally are observed above the threshold](#) (Tromp-Van Meerveld and Mcdonnell, 2006; Zehe et al., 2007; Wei et al., 2020). [A unified threshold-based hydrological theory that possibly advanced catchment hydrology was extensively discussed during AGU 2011 Fall Meeting](#) (Ali et al., 2013), [and later was continuously developed](#) (Ross et al., 2021; Ross, 2021; Ali et al., 2015; Scaife et al., 2020). [Theoretical advancements in hydrology can support](#) the development of appropriate algorithms for [more efficient](#) predictive hydrologic models.

The process [of threshold behavior generally shows](#) different nonlinear shapes of hydrological [response](#) for a storage-discharge relationship (Ali et al., 2013; Wang et al., 2022), such as [the Hockey stick, Step or Heaviside function, Dirac function, and Sigmoid function](#). [The transition from below-threshold to above-threshold behavior for different diagnostic shapes suggests several mechanisms of water retention and release in the watershed](#). [In the literature, the runoff behaviors with Hockey stick shape were found](#) at the hillslope (Tromp-Van Meerveld and Mcdonnell, 2006; Fu et al., 2013b; Wang et al., 2022)(Tromp-Van Meerveld and Mcdonnell, 2006; Fu et al., 2013a; Wang et al., 2022) and watershed scales (Wei et al., 2020; Farrick and Branfireun, 2014; Scaife and Band, 2017; Buttle et al., 2019; Zhang et al., 2021b). For example, Farrick and Branfireun (2014) identified a

设置了格式: 非突出显示

设置了格式: 非突出显示

设置了格式: 字体:(默认) Times New Roman, (中文) Times New Roman, 非突出显示

设置了格式: 非突出显示

设置了格式: 非突出显示

设置了格式: 非突出显示

设置了格式: 非突出显示

设置了格式: 非突出显示

设置了格式: 字体: Times New Roman

设置了格式: 非突出显示

设置了格式: 非突出显示

设置了格式: 非突出显示

设置了格式: 非突出显示

设置了格式: 非突出显示

threshold value of 289 mm of gross precipitation (P) and antecedent soil water index (ASI) in a forested catchment of 3.15 km² in Mexico, which presented the threshold behaviors with two-linear runoff response controlled by subsurface stormflow mechanism. While it seemed to follow the Hockey stick shape, above-threshold's stormflow amounts showed high variability (Scaife and Band, 2017; Zhang et al., 2021b). The phenomenon possibly increased the uncertainty of prediction for higher stormflow amounts and flood disasters. Wei et al. (2020) proposed a rainfall-runoff relationship as having multiple thresholds with intervening linear segments to reflect the initial streamflow activation and larger flood response. Understanding the change from slow to rapid stormflow response and larger flash flood hydrograph is vital. However, a clear picture of the physical connotations of threshold behaviors associated with the generation and development of flash flooding is still missing (Wei et al., 2020).

Hydrologic threshold signatures at the catchment scale, as a new diagnostic tool, can effectively evaluate the long-term variations in stormflow response to forest recovery following natural disturbances (Wei et al., 2020; Ali et al., 2013; Scaife and Band, 2017). Natural disturbances in hydrology and associated effects are summarized in Table 1 and categorized into acute disturbances (AD) and chronic disturbances (CD). Acute disturbances, which are abrupt or sudden, such as earthquakes, wildfires, snow and ice, volcanic activity, etc. (Table 1), tend to trigger the most drastic hydrological response and alter the hydrological regime after the disturbance. Comparatively, chronic disturbances (Table 1), which are more gradual and mostly affected by climate change (Hwang et al., 2018; Scaife and Band, 2017; John et al., 2022; Seidl et al., 2017), generally lead to a progressive reduction in forest canopy without immediate destruction of soil-root system and bedrock (Bladon et al., 2019; Hoek Van Dijke et al., 2022). Abrupt disturbance events could significantly alter the original landscape configuration and structure as well as the vegetation-soil system (Figure 1), readily resulting in high peak flows and catastrophic flash flood disasters (Arheimer and Lindström, 2019; Hoek Van Dijke et al., 2022).

For instance, the famous Wenchuan earthquake on 12 May 2008 triggered numerous coseismic landslides of nearly 2.0×10^5 (Fan et al., 2018; Xu et al., 2013), leading to the rapid and widespread destruction of vegetation-soil structure and fragment rock mass structures (Cui et al., 2012; Zhang et al., 2021a). These disruptions can reduce the canopy interception and shallow soil water storage capacity, increasing more throughfall precipitation reaching the soil surface and subsurface stormflow magnitudes contributing to the flash flood hydrograph (Zhang et al., 2018).

After the abrupt disturbance, the exposed bedrock in the trailing edge of the landslides easily induced the Horton overland flow, and the generated loose deposition in the lower part of the landslides generally increased subsurface stormflow with the microporous flow (Mirus et al., 2017a; Zhang et al., 2018). Such hydrological behaviors are related to the quick runoff generation mechanism with a short lag time, resulting in higher runoff potential (Figure 1). However, the hydrological signature (e.g. soil water movement and stormflow generation) of risky landslides within steep hillslopes was not easy to capture.

During the recovery processes, the earthquake-derived amounts of geohazards affected by large rainstorms led to unstable forest shrinkages and landslide expansions (Figure 1) at long-term timescales in a forest-dominated mountainous watershed. The unstable disturbances from endogenous (earthquake) and exogenous (rainstorms and concomitant hydro-geohazards) origins remarkably increased the uncertainty in the assessment of the hydrological regime from disturbance to recovery and flood risk management (Seidl et al., 2017). Previous studies have suffered from over-

城代码已更改

城代码已更改

calibrated hydrological models (Tunas et al., 2020; Maina and Siirila-Woodburn, 2019; Chiang et al., 2019) and a lack of understanding of runoff generation mechanisms in exploiting the effects of natural disturbance events on streamflow response. The efficient identification of nonlinear hydrologic behaviors in an earthquake-affected watershed as well as the understanding of post-earthquake long-term dynamics of hydrologic threshold patterns is still urgently needed.

Table 1: Category and Summary of Natural Disturbances in Hydrology and Associated Effects

Disturbance Agent	Category	Location	Method	Disturbance effects	References
Insect infestation	CD	Oregon in the USA	Field monitoring	Interception, streamflow, evapotranspiration, energy balance	Bladon et al. (2019)
Drought		Rocky Mountain in the USA	Remote sensing; Field monitoring and laboratory measurements	Flow path, stream chemistry, peak flow, forest productivity	Knowles et al. (2017); Murphy et al. (2018)
Invasive species		Colorado in the USA	Field monitoring	Water resources, interception, soil intention	Brantley et al. (2013)
Peatland degradation		Finland	Field measurements	Streamflow, water table, stream chemistry	Menberu et al. (2016); Shuttleworth et al. (2019)
Snow and ice	AD	Guangdong in China	Field monitoring	Interception, peak flow	Wei et al. (2020)
Wildfire		Colorado in the USA	Numerical Modeling, Field monitoring and laboratory measurements	Infiltration, interception, erosion, sediment yield, water quality, peak flow	Moody et al. (2013); Ebel (2020)
Volcanic activity		Mount St. Helens in Washington; Patagonia in Chile	Field monitoring and laboratory measurements	Sediment yield, infiltration, runoff, peak flow	Major and Mark (2006); Pierson et al. (2013)
Typhoon		Tacloban in Philippines	Field monitoring and laboratory measurements	Landslides, interceptions, peak flow	Zhang et al. (2018);
Earthquakes		Taiwan in China, Indonesia Sichuan Province in China	Numerical Modeling, Remote sensing, Field monitoring	Landslides, sediment yield, interceptions, peak flow, groundwater level, baseflow	Montgomery and Manga (2003); Tunas et al. (2020); This study

Notes: CD and AD are chronic disturbance and acute disturbance, respectively.

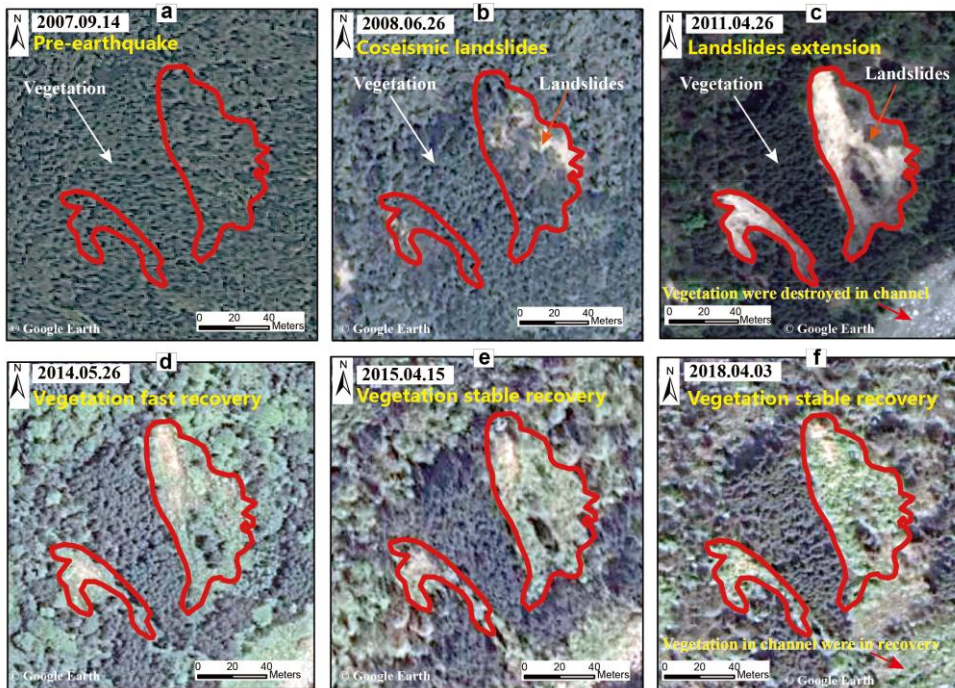


Figure 1: Long-term evolutions of landslides in a disturbed watershed pre- and post-Wenchuan earthquake disturbance.

Additionally, the scarcity of long-term hydrometeorological observation data as well as the inaccessibility of post-earthquake roads is a limitation to understanding the flood response driven by acute disturbance. In this study, the relationship between antecedent soil water storage, rainfall, and runoff at a 5-min interval in an earthquake-affected watershed was investigated. To understand the long-term variations in the hydrologic regime affected by an earthquake and their dominant controls, the hydrologic thresholds of precipitation + antecedent soil moisture were proposed. The specific objectives of this study are: (1) to examine the heterogeneity in hydrologic thresholds in undisturbed and disturbed lands; (2) to identify how the subsurface stormflow and variable source area affected by the earthquake-induced landslides control heterogeneity in the non-linear physical processes from rainfall to runoff at the watershed scale; and (3) use of integrated threshold behaviors and linear runoff response to gain insight into the long-term dynamics and nonstationarity of hydrological behaviors affected by the interactions of post-earthquake landslides and vegetations evolution. Assessment of streamflow regime and flood risk could benefit from the effectively identifying the hydrological threshold signatures that mainly affect a watershed's streamflow response (Ali et al., 2013; Zhang et al., 2021b; Ross et al., 2021).

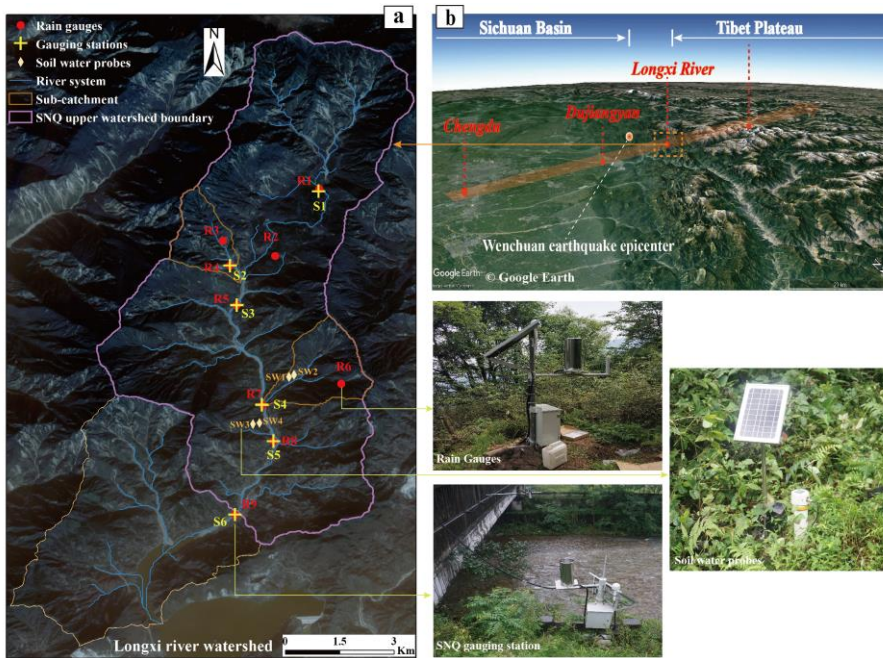
- 设置了格式: 非突出显示
- 设置了格式: 非突出显示
- 设置了格式: 非突出显示
- 设置了格式: 非突出显示
- 设置了格式: 非突出显示
- 设置了格式: 非突出显示
- 设置了格式: 英语(英国)

120 **2 Data and methods**

2.1 Study area

This study was carried out in a 78.3 km² forested Longxi River (LXR) Experiment Watershed, eastern Tibet Plateau, China (Figure 2). The forest land occupied 96.9% of the whole watershed area before the 2008 Wenchuan earthquake (Zhang et al., 2021a), mainly consisting of *canopy conifer*, *dark coniferous*, and *broad-leaf forests*. After the earthquake, the forest land had a 19.9% shrinkage percentage (Zhang et al., 2021a). The post-earthquake hydro-geohazards, such as landslides and debris flows, could lead to an unstable recovery trend of landscape vegetation (Figure 1), significantly influencing the stability of hydrologic function and stormflow behaviors of the watershed from rainfall to runoff (Zhang et al., 2021a).

设置了格式: 无下划线



130 **Figure 2:** Longxi River (LXR) watershed (78.3 km²) located in the eastern margin of the Tibet Plateau (a-b), affected by the 2008 Wenchuan earthquake, and the detailed monitoring stations, mainly comprising rain gauges (R1-R9), gauging stations (S1-S6) and soil water probes (SW1-SW4).

The soil types mainly consist of Haplic Luvisols, Chromic Luvisols, Dystric Cambisols, and Haplic Alisols. Surface soil hydraulic conductivity in forest land is high, with values of 10-200 mm/h (Zhang et al., 2021b). Subsurface stormflow generated on the soil-bedrock interface under heavy rainfall conditions is a dominant runoff sources contributing to flash flooding (Zhang et al., 2021b). The elevation in the region ranges from 870 to 3284 m asl with high relief. The strong orographic effect generally leads to more rainfall amounts in steep mountainous watersheds (Figure 2b), readily leading to large flood disasters. In the earthquake-affected regions, analyzing the disturbance-recovery processes of landscape vegetation will contribute to understanding potential long-term evolutions in mechanisms of runoff generation and flash flood disasters.

2.2 Hydrometric observations

Open field precipitation from nine rain gauges was automatically recorded at a 5-min interval (Figure 2a), and the flow discharge with high flow velocity and water level during the flood hydrograph was monitored at a 5-min interval and calculated based on the hydraulic Entropy's method (Chen, 2012; Moramarco et al., 2004; Bahmanpouri et al., 2022; Zhang et al., 2021b). Volumetric soil moisture content (θ) was recorded at a 5-min interval using the soil water probes (Zhang et al., 2021b). Each probe equipped with eight sensors at a 10 cm depth interval was installed 80 cm in soil profiles below the surface (Figure 2a). The monitored probes (SW1) and (SW2) at upslope and downslope topographic positions were located in an undisturbed forest and grass-shrub lands, and SW3 and SW4 were located at a disturbed landslide. The depth equivalent antecedent soil water index (DASI) at the start of each rainfall event was obtained (Zhang et al., 2021b), which was indicative of the initial shallow soil water storage (Wei et al., 2020).

2.3 Definitions of storm events and hydrologic thresholds

Storms are defined as events with > 4 mm of precipitation, separated by more than 6 h (Farrick and Branfireun, 2014; Penna et al., 2011). A total of 47 events in this experimental watershed were identified during periods of June ~ August from 2018 to 2020, possibly filtering out the uncertainty in assessing hydrological behaviors from seasonal variations of the vegetation forest canopy (Hwang et al., 2018). For each event, the stormflow (Q_s) is separated from the flood hydrograph using a proposed two-parameter recursive digital filter method (Eckhardt, 2005; Zhang et al., 2021b). The catchment threshold behaviors were quantitatively assessed using piecewise regression analysis (PRA), and the hydrologic threshold values and slope parameters from each linear segment of the PRA function were calculated (Zhang et al., 2021b; Oswald et al., 2011). The different breakpoints and slope parameters of PRA might contribute to understand the broad controls of shifts from slow to fast stormflow response and flash flood disasters (Zhang et al., 2021b; Scaife and Band, 2017; Oswald et al., 2011). Uncertainty in visually assessing hydrological thresholds is typically increased by nonlinear and complex stormflow

设置了格式: 字体: 非倾斜

behaviors (Detty and Mcguire, 2010). However, the automatic identification of thresholds and linear slope parameters with a maximum likelihood approach (Muggeo, 2003) could be effective.

2.4 Determination of nonstationarity in pre- and post-earthquake threshold behaviors

To clearly understand long-term threshold evolutions and emergent behaviors variations pre- and post-earthquake at the watershed scale, an *integrated watershed average (IWA)* index for the thresholds was proposed to characterize the watershed stormflow emergent behaviors. The *IWA* index mainly considers the processes of runoff generation in the watershed's underlying surface based on the principle and framework of runoff potential for curve numbers (Deshmukh et al., 2013). The underlying surface mainly comprises the land use types, the shallow watershed storage capacity and physical properties in soils at different locations, and bedrock types. These factors play vital roles in the processes of runoff generation. Another dominant water source of event precipitation amounts in the atmosphere is also taken into account. Therefore, the index is mainly calculated from the area contribution ratio of different land use types (R_i), the shallow water storage capacity at different locations ($DASI_i$), and event precipitation amounts (P) as

$$T_{i-IWA}(x) = \sum_{i=1}^n R_i * x_i = \sum_{i=1}^n \frac{a_i}{A} * (DASI_i + P) \quad (1)$$

where $DASI_i$ is the initial shallow storage capacity of the i th land-use type in the underlying surface (mm), P is the event precipitation (mm), x_i is the runoff generation threshold or rising threshold for the i th land-use type (mm), a_i is the area of the i th land use type (km^2), A is the watershed area of the study area (km^2), R_i is the ratio of a_i and A (%), and n is the number of land use types, $T_{i-IWA}(x)$ is an integrated watershed average index for the thresholds. Water bodies, building up and roads are assumed to be impermeable, and the initial storage capacity is assumed to be 0. Based on equation (1), $T_{i-IWA}(x)$ could be calculated to identify and compare the pre- and post-earthquake variations in thresholds behaviors at a watershed scale, reflecting the hydrological effects under the long-term interaction and development of the post-earthquake vegetation-hydrogeological hazards.

3 Results

3.1 Stormflow Threshold Behaviors

The collected event precipitation amounts (P) from a series of 40 large storm events ($P > 10\text{mm}$) (Zhang et al., 2021b) showed a great variation from 16.4 to 263.9 mm. At the larger P values, the stormflow amounts (Q_q) generally had a very large variability (Zhang et al., 2021b; Farrick and Branfireun, 2014), increasing the uncertainty in the estimation of the rainfall-runoff relationship. No significant linear statistical relationship between $DASI$ and Q_q was found in all monitored sites ($p > 0.05$, $r^2 \leq 0.017$, see Zhang et al. (2021b)). Once the $DASI$ was combined with P , a more visually evident three-nonlinear threshold behavior for the relationship of $DASI+P$ and Q_q ($p < 0.001$) was observed with two hydrologic thresholds or breakpoints of

each location (Figures 3), i.e., generation threshold (T_g) and rising threshold (T_r).

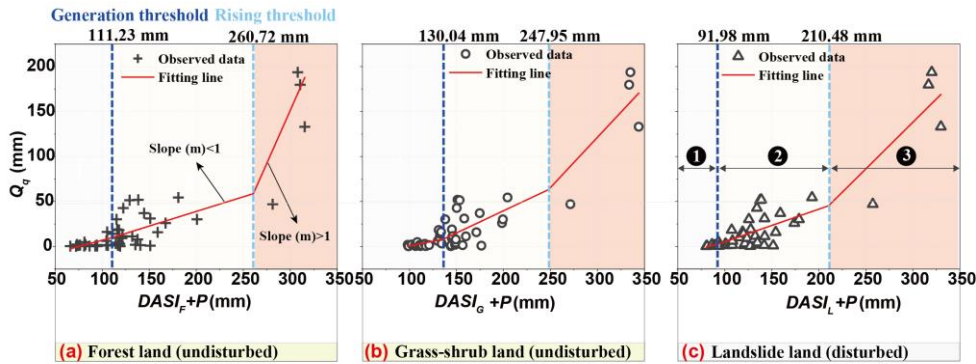


Figure 3: The piecewise regression analysis of event stormflow amount (Q_g) plotted against the sum of event precipitation amounts (P) and $DASI$ at the forest (a), grass-shrub (b), and landslide (c) lands. The undisturbed forest and grass-shrub lands represent the pre-earthquake period, as reported by Zhang et al. (2021b), and the disturbed landslide land represents the post-earthquake period. Redlines indicate the liner fitting for the piecewise regression for the variable of $P + DASI$ at the confidence level of 95%.

Additionally, significantly lower values in both T_g (91.98 mm) and T_r (210.48 mm) were observed in monitored landslide land (Table 2 and Figure 3). The threshold values in T_g and T_r in landslide decreased by up to 28.84 mm and 43.86 mm, respectively, compared to those average values in the undisturbed forest and grass-shrub lands. This indicates a lower post-earthquake threshold with response metric pairs that can lead to large flash flood disasters. The slope parameters from m_{i1} to m_{i3} were different by an order of magnitude (Table 2). A lower value of m_{i1} mainly depicts a more gradual process of runoff generation. Observed larger storms in the third phase readily led to higher m_{i3} values of >1 , indicating fast stormflow response during flash flood hydrograph. For different land-use types, lower m_{i3} values occurred in monitored landslide land. It was mainly owing to the deficiency of vegetation canopy and soil water storage capacity, highlighting the contribution of watershed storage during the first and second phases to the abrupt response of flash flooding in the third phase.

Table 2: Comparison of parameters in assessing the three-linear threshold behaviors of $DASI+P$ and Q_g relationships at the confidence level of 95%

Location	Period	Parameters						
		T_g (mm) ^{±s2}	T_r (mm) ^{±s2}	$m_{i1}T_r$ (mm)	$m_{i2}T_r$	$m_{i3}T_r$	r^2 ^{±s2}	SEE ^{±s2}

格式化表格

Forest land	Pre-earthquake [#]	<u>111.20.88[±]</u>	<u>260.7411.2</u>	<u>0.28260.7</u>	<u>0.330.28</u>	<u>2.360.33</u>	<u>0.88^{**}</u>	<u>17.170.88[±]</u>
Grass-shrub land		<u>130.40.84[±]</u>	<u>247.9430.4</u>	<u>0.21247.9</u>	<u>0.490.21</u>	<u>1.120.49</u>	<u>0.84^{**}</u>	<u>15.650.84[±]</u>
Landslide land	Post-earthquake	<u>91.980.87[±]</u>	<u>210.4891.98</u>	<u>0.24210.4</u>	<u>0.360.24</u>	<u>1.040.36</u>	<u>0.87^{**}</u>	<u>16.540.87[±]</u>

Note:

m_{ij} indicates the values in the slope parameter of PRA equations from the j_{th} phase at the i land (i =forest, grass-shrub, and landslide lands, j =1, 2, 3 shown in Figure 3).

215 [#] denotes the collected data in a row, reported by Zhang et al. (2021b).

^{**} indicates that correlation is significant at the 0.01 level (two-tailed).

SEE is the standard error of estimate in multiple regressions.

3.2 Threshold Pattern Variations at an Earthquake-Affected Watershed

220 Due to the fragmentation and patchiness of the post-earthquake watershed underlying (Zhang et al., 2021a; Yunus et al., 2020) and unevenness of monitoring locations for different land use (Farrick and Branfireun, 2014), the assessment of the hydrological threshold behavior at the watershed scale is largely uncertain and non-stationary. The scarcity in of hydrological information before a large earthquake and road unreachability of post-earthquake disturbed regions increase the difficulty of late monitoring in earthquake-affected watersheds (Mirus et al., 2017b; Zhang et al., 2021b). It limited our knowledge about how the abrupt earthquake affects the stormflow threshold behavior at the watershed scale.

225 The integrated watershed average (IWA) index for both two thresholds was calculated using equation (1) to characterize the long-term changes in stormflow threshold behaviors pre- and post-earthquake disturbance. Significant lower values in T_{g-IWA} and T_{r-IWA} were found during post-earthquake periods (Figure 4a) and the lowest values (109.34 mm and 250.72 mm) of both occurred in the co-seismic phase. Within 3 years (2008~2011) after the earthquake, the values of both thresholds values remain low due to the unstable evolution of post-earthquake hydrogeological hazards (Zhang et al., 2021a; Shen et al., 2020). After the key tipping-turning point in 2011, they they recovered rapidly within 3-5 years (2011~2013) after the earthquake and then gradually stabilized and approached the pre-earthquake level. A significant negative correlation relationship ($p<0.05$) between hydrologic thresholds and peak discharges was obtained served Both thresholds varied just the opposite of these simulated interannual variations in peak discharge and flood volume (Figure 4b), which was reported by observed data combined with a hydrological model from Zhang et al. (2021a) in this experimental watershed, (Figure 4b). Shortly after the earthquake, a significantly lower average value with ~9 mm of T_{r-IWA} at the watershed scale increased peak discharge and flood volume by up to 22.58% and 25.15%, respectively (Table S1). This indicated that the lower values in generation and rising thresholds after the earthquake require less watershed storage capacity (rainfall and antecedent soil content) input to readily triggered the huge flash flood occurrence. Figures 4a and b show the variation from 2007 to 2018 of in the stormflow threshold behaviors

设置了格式: 字体: 10 磅

设置了格式: 字体: 倾斜

设置了格式: 字体: (中文)+中文正文(宋体), (中文) 中文(中国)

设置了格式: 字体: 倾斜

设置了格式: 非突出显示

设置了格式: 非突出显示

240 and event flood response. Four phases were observed during the hydrological disturbance-recovery process, effectively and
 245 rationally predicting the flood regimes associated with stormflow threshold behaviors due to earthquake disturbance.

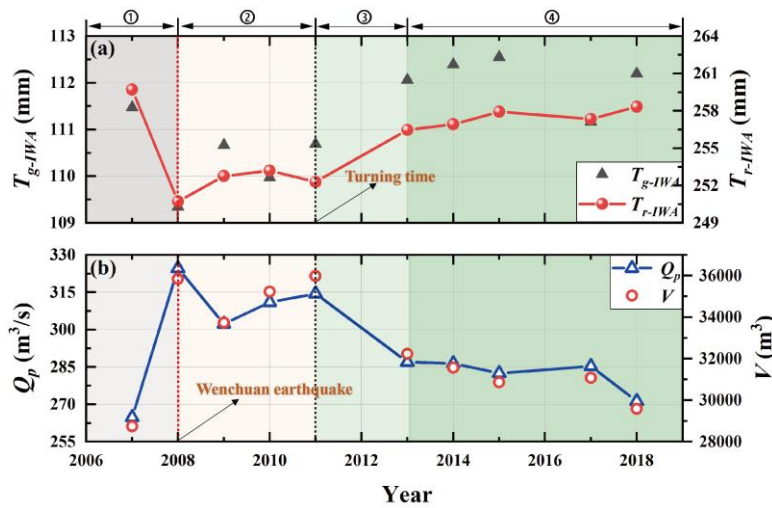


Figure 4: Changes in (a) observed stormflow threshold behaviors, including integrated watershed generation threshold (T_{g-IWA}) and rising threshold (T_{r-IWA}), and (b) a large flood event response selected from Zhang et al. (2021a) during the periods of 2007 ~ 2018 before and after the earthquake, including peak discharge (Q_p) and flood volume (V). ① (2007-2008): T_{g-IWA} and T_{r-IWA} abruptly decrease and peak discharge rapidly increases; ② (2008-2011): T_{g-IWA} and T_{r-IWA} contain low values triggered by the overlapping of post-earthquake active geohazards; ③ (2011-2013): T_{g-IWA} and T_{r-IWA} abruptly increase and peak discharge rapidly decrease; ④ (2013-2018): the hydrologic variables gradually stabilized and approached the pre-earthquake level.

250 4 Discussion

4.1 Controls on Threshold Behaviors

Those threshold behaviors and nonlinear stormflow responses at the watershed scale are useful for understand the generation and development of flash floods (Zhang et al., 2021b; Wei et al., 2020). They might supplement the threshold-based hydrological theoretical framework (Ali et al., 2013). To extend the application and efficacy of the derived T_g and T_r , three large flood events (2019-08-19, 2020-08-15, and 2020-08-29, see Figure 5), with the variation in rainfall intensity (I_{5min}), event accumulative precipitation (EAP) and discharge (Q) at a 5-min interval, were further considered. The T_g value (120.8 mm) was observed during the rapid streamflow change, and the abrupt change in stormflow and flood response was

设置了格式: 字体: 倾斜

设置了格式: 字体: 倾斜

设置了格式: 字体: 倾斜

设置了格式: 字体: 倾斜

设置了格式: 字体: 倾斜

设置了格式: 字体: 倾斜

readily stimulated at the threshold of T_r with the value of 254.3 mm (Figure 5). Such emergent behavior and signatures at the watershed scale demonstrated the presence of the critical points in time and space where runoff response rapidly changed (Ali et al., 2013; Zhang et al., 2021b). The threshold index was efficiently verified through the applications of the magnitudes in two threshold values during the flood hydrograph (Figure 5) and their concomitant hydrological variations with the discharges derived from runoff potential (Figure 4). However, we also acknowledge a limitation that only the dominant hydrological process of runoff generation was considered while the important confluence flow was mostly ignored. In a future study, such metrics will be involved in the runoff generation and confluence flow to more efficiently reflect the watershed's hydrologic behavior.

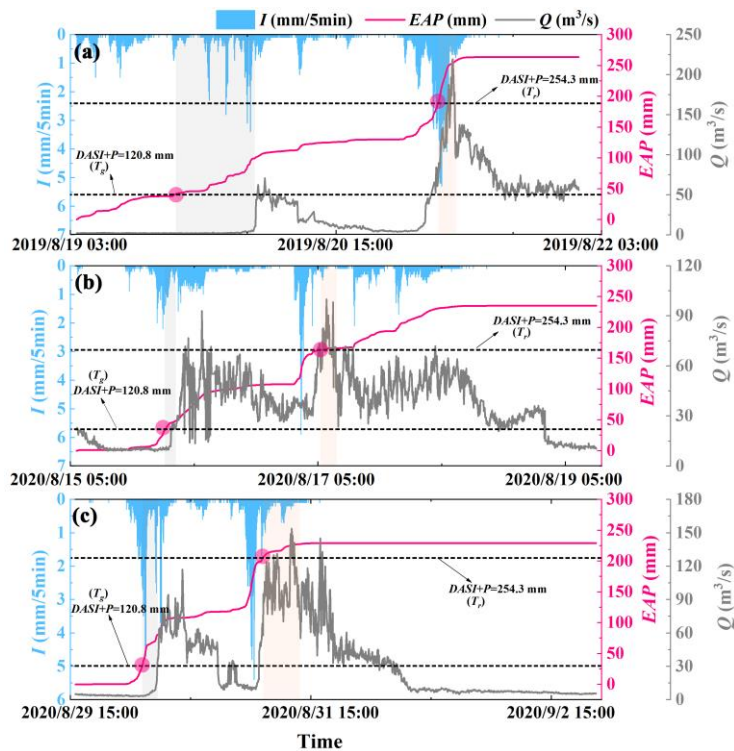
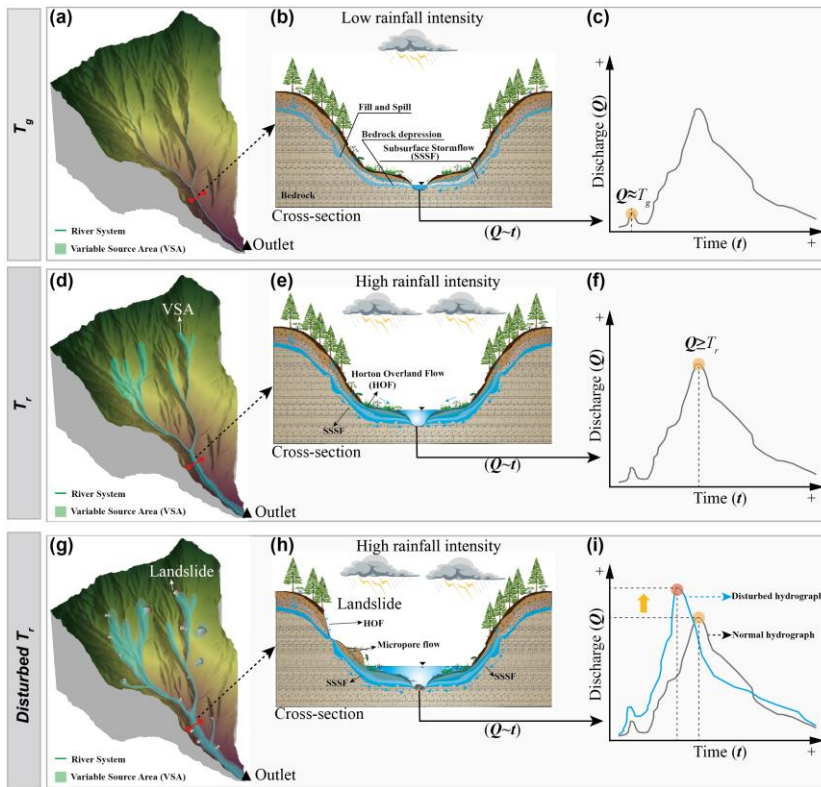


Figure 5: Generation and development of the flash flood hydrograph (a: 2019-08-19 event, b: 2020-08-15 event, c: 2020-08-29 event) with the variation in 5-min rainfall intensity (I_{5min}), event accumulative precipitation (EAP), and flow discharge (Q) based on the derived generation threshold (T_g) and rising threshold (T_r).

270 The nonlinear shape of storage-discharge relationships could reflect the runoff-generating mechanisms underlying the retention-release processes of event water input at the watershed scale (Kirchner, 2009; Ali et al., 2013), efficiently diagnosing the inherent change in watershed nonlinear hydrologic behavior. Above the critical threshold value, a rapid discharge response could be significantly observed in Figure 3. It has been demonstrated that bedrock depression storage in the soil-bedrock interface (Fu et al., 2013b; McDonnell et al., 2021) and soil moisture deficit (Cain et al., 2022; Zhang et al., 2021b; Fu et al., 2013a) are the main factors controlling the initial emergent behavior and threshold properties (T_g) of rainfall-runoff. Some common characteristics associated with process-based interpretation are highly permeable soils and low permeability of bedrock at the hillslope with steep slopes (Tromp-Van Meerveld and McDonnell, 2006; Farrick and Branfireun, 2014; Scaife and Band, 2017; Ross et al., 2021). These properties generally lead to a significant soil-rock interface, readily triggering the subsurface stormflow on the interface under heavy rainfall conditions. At the T_g value (120.8 mm), bedrock depressions on the hillslope could be filled with water from rapid rainfall infiltration while water spilled over the undulating soil-bedrock interface (Figure 6a). The subsurface stormflow and partly saturated areas (i.e., variable source area) were initially connected to the channel under cumulative rainfall conditions (Farrick and Branfireun, 2015), improving the connectivity of stream-adjacent hillslope hydrological processes and activating the higher streamflow (Figure 6b-c). Once above the T_r value, the variable source areas (VSA) close to the channel or impermeable surface under high rainfall intensity showed a significant expansion (Figure 6d). Below and above the generation and rising thresholds, the changes in minimum contributing area (MCA, with mean values of 13.79 km², 22.52 km², and 34.43 km², respectively) and stormflow discharge (Q_g , with mean values of 3.14 mm, 22.5 mm, and 138.3 mm, respectively) are significant (Zhang et al., 2021b; Dickinson and Whiteley, 1970). Higher values of MCA above the rising threshold exceeded 60% of the watershed area (Zhang et al., 2021b), significantly increasing the hydrological connectivity of hillslope riparian-stream and readily facilitating the occurrence of catastrophic flash flood disasters (Figure 6e-f).

The abrupt flow process was mainly affected by subsurface stormflow and Horton overland flow generations at the foot of the slope subjected to storm size and intensity rather than antecedent soil moisture (Zhang et al., 2021b; Farrick and Branfireun, 2014).



295

Figure 6: Schematic diagram showing the changes in watershed variable source area (a, d, g), hillslope runoff process at the cross-sections (b, e, h), and flow discharge hydrographs (c, f, i) at the generation threshold (T_g), rising threshold (T_r), and T_r by affected by the earthquake-induced landslides, respectively.

300

Figure 6g shows the large expansion of VSA related to landslides which generally destroy the crown canopy, litter layer, and root-soil system in hillslopes (Chiang et al., 2019; Zhang et al., 2021a). These destructive processes alter the original landscape, with the formation of bare rock with steep slopes and accumulations of loose materials. For instance, the Wenchuan earthquake-induced $\sim 2.0 \times 10^5$ landslides decreased by $\sim 30\%$ the forest coverage (Cui et al., 2012), altering the infiltration runoff processes and the contribution of Horton overland flow and subsurface stormflow to flood hydrograph in the channel (Hong et al., 2010; Ran et al., 2015; Sidle et al., 2017) (Figure 6h). Zhang et al. (2021a) applied hydrological model and field observations to demonstrate that the landslides-induced bare land can increase by $>10\%$ of the runoff potential at the watershed

305

scales if compared to that before the earthquake. Peak discharges increased by 22.58%~367.42% and the time to peak was advanced by 25 min. This is almost consistent with Tunas et al. (2020) in the Bangga River Basin affected by the 2018 Palu Earthquake in Indonesia. The large physical disturbances triggered by earthquake-induced landslides can efficiently reflect the reduced water storage of shallow soil and vegetation canopy. The post-disturbance stormflow thresholds can show a lower value (Table 2), and require less water input into the underlying surface to activate the runoff generation and flash flooding.

4.2 Nonstationary Hydrological Behaviors Triggered by Earthquake

Strong earthquake-induced landslides can severely fragmentize original landscape ecosystem but with spatially uneven distribution characteristics, such as the back-slope effect (Wang et al., 2019; Xu et al., 2011; Zhang et al., 2021a), hanging wall effect (Huang and Li, 2009; Beyen, 2019), distance effect along the earthquake fault zone (Xu et al., 2011), etc. These spatially unbalanced conditions generally led to apparent uncertainty and non-stationarity in hydrologic response and runoff generation in the earthquake-affected regions, severally affecting the identification and judgment of the formation and development of flash floods. Zhang et al. (2021a) first illustrated the change in runoff response on both sides of the Longxi River watershed due to the back-slope effect. They found that the landslide area density of 13.76% on the right bank during the coseismic period was approximately three times that (4.84%) on the left bank, exhibiting an undulating but unpredictable disturbance–recovery process. This phenomenon highlighted the importance of spatially uneven distribution and dynamic nonstationarity at timescales of earthquake-induced landslide patches for an accurate assessment of the runoff generation and the dynamic evolution of catastrophic flash flood.

Interannual variations of rainfall-runoff relationships manifest a slow undulating increase in thresholds after the earthquake (Figure 4a), predicting the short- and long-term changes and nonstationarity in stormflow behaviors at long timescales. These long-term, nonunique interannual thresholds indicated that stormflow behaviors at the watershed scale are closely related to catchment geophysical characteristics (Oswald et al., 2011) or climate (Graham and McDonnell, 2010), changing vegetation dynamics (Hwang et al., 2018) as well as natural disaster disturbance (Ebel and Mirus, 2014). Also, at event timescales, greater thresholds (T_r) generally occurred during wetter growing seasons (Scaife and Band, 2017; Wei et al., 2020). Above the T_r , the catastrophic flash flood disasters were readily triggered by summer high-intensity convective storms that possibly activate preferential soil flows facilitating greater and faster stormflow generation in the shallow subsurface (Zhang et al., 2021b). This is associated with the lateral extension of hillslope-channel hydrological connectivity (Farrick and Branfireun, 2014; Ross et al., 2021), abruptly increasing the VSA at the watershed scale.

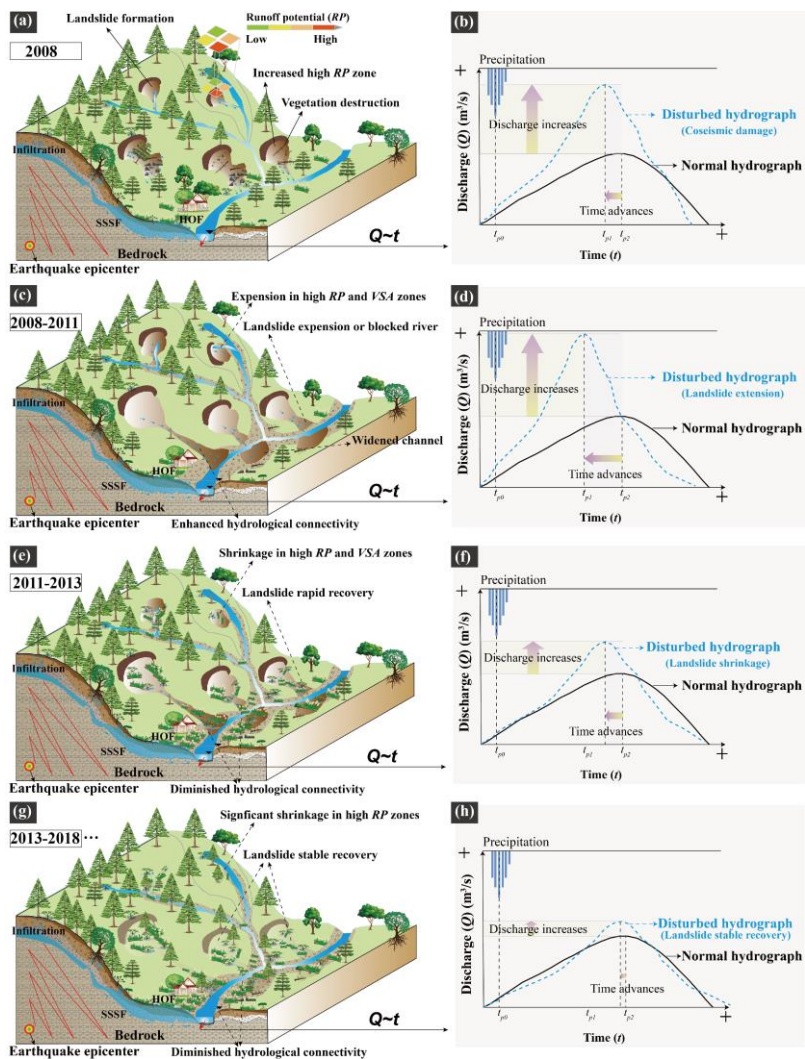


Figure 7: Conceptual model explaining the long-term interactions in disturbed hydrological behaviors during the formation-development-recovery process of the landslides after the Wenchuan earthquake.

By filtering out the influence of climate variables at event timescales, the effects of earthquake disturbance on flash flood hydrographs were evaluated to determine how long-term interactions of earthquake-induced landslides and vegetation might alter interannual stormflow thresholds. Figure 7 presents a conceptual model of the long-term evolution and interaction in disturbed hydrological behaviors, affected by the unsteady formation-development-recovery processes of the landslides after the earthquake. The Wenchuan earthquake largely destroyed the original landscape and vegetation-soil ecosystem triggering hydro-geohazards (Cui et al., 2012; Ran et al., 2015; Shafique, 2020; Zhang et al., 2021a). After the earthquake, the larger landslides with exposed bedrock and loose deposition can lead to more expansion of higher runoff potential (*RP*) and *VSA* zones (Figure 7a). It is related to the Horton overland flow and subsurface stormflow with the microporous flow of the landslides. Their processes facilitate quick runoff generation contributing to flood hydrograph.

The generation (T_g) and rising (T_r) thresholds associated with vegetation canopy interception and antecedent wet conditions (Wei et al., 2020) were significantly lower after the earthquake (Table 2 and Figure 4a), readily leading to a larger flood peak discharge and a shorter time to peak (Figure 7b). Due to the complex geo-hazards processes, the destruction of the vegetation-soil ecosystem and widen channel further expanded the high *RP* and *VSA* zones, and enhanced the structure hydrological connectivity shown in Figure 7c (Moreno-De-Las-Heras et al., 2020). The value in T_r related to the large flash floods drastically decreased (Figure 7d), generating higher peak discharge and less lag time. After the key turning point in 2011, the rapid recovery of landslide and vegetation-soil ecosystem was observed from 2011 to 2013 (Figure 7e-f). During the period, the *RP* and *VSA* zones rapidly expanded while the hydrological threshold behaviors were quickly recovered and improved. Our findings emphasize the importance of earthquake-induced landslides and vegetation dynamics on event- and long-term scale stormflow response, but more research is required to fully understand the disturbed hydrological behaviors and threshold-based hydrological theoretical framework.

4.3 Challenges in Identifying Nonunique Threshold Behaviors disturbed by Large Disaster Events

Abrupt disturbance events generally disrupt the hydrologic storage and functional connectivity at spatial and temporal scales (Ebel and Mirus, 2014), readily leading to the nonunique thresholds in nonlinear behaviors of rainfall-runoff processes (Arheimer and Lindström, 2019; Scaife and Band, 2017). Uncertainties and challenges in characterizing the nonunique threshold behaviors from disturbance hydrology perspectives still need to be clarified.

- (1) The lack of detailed observation data about hydrologic fluxes and subsurface storage dynamics before and after an abrupt event is a significant limitation to understanding the variations in flow pathways and runoff generation mechanisms (Farrick and Branfireun, 2014; Ebel, 2020; Chiang et al., 2019). It will be difficult to accurately identify the presence and

设置了格式: 字体: (默认) + 西文正文 (Times New Roman)

370 the form of hydrological threshold signatures that influence a watershed's streamflow response, possibly leading to the assessment uncertainties of the flood hydrologic regime.

(2) The watershed spatially [broken](#) patchiness and dispersion brought on by the occurrence of sudden events are very evident (Zhang et al., 2021a; Sidle et al., 2017; Wang et al., 2019), but the methods to quantitatively assess the variable functional hydrologic connectivity associated with runoff generation mechanisms are still lacking (Bracken et al., 2013; Beiter et al., 2020). This limits our understanding of the sole hydrological responses and variable threshold behaviors by filtering out the effect of loose materials on flooding in the disturbed regions.

375 (3) Heterogeneity in the regional plant community composition and subsurface critical zone thickness related to water storage capacity (Hahm et al., 2019; Shangguan et al., 2017; García-Gamero et al., 2021) generally leads to different runoff generation mechanisms and nonstationary threshold behaviors in different climate zones. A reasonably generalized ecohydrological zoning with some organizing principles or frameworks could be a better road towards a unified threshold-based hydrology theory proposed by Ali et al. (2013), further facilitating the cross-site syntheses and validation.

5 Conclusions

This study offered insight into the complex interactions of hydrological processes at a small disturbed, forested experimental watershed by revealing relatively simple, generalized nonlinear runoff behaviors. An integrated response metric pair was applied to identify stormflow threshold behaviors and evaluate the long-term threshold dynamics after the Wenchuan earthquake disturbance. Lastly, we revealed the subsurface stormflow and variable source area as dominant controls on the dynamics of threshold behaviors pre- and post-acute disturbance rather than chronic disturbance. Conclusively the key findings mainly are:

(1) Lower values in both generation and rising thresholds derived from nonlinear stormflow behaviors generally occur in disturbed landslide regions, which is [easier](#) to lead to large flash flood disasters.

(2) The dynamics of [two](#) thresholds through a novel integrated watershed average index can characterize the hydrological disturbance-recovery process before and after an abrupt earthquake.

390 (3) [The runoff generation mechanisms of subsurface stormflow and variable source area mainly control the](#) non-stationarity in threshold behaviors and linear stormflow response. This is related to the largely spatially [heterogeneous](#) distribution of abrupt earthquake-induced landslides and temporally undulating recovery of disrupted landscape and vegetation-soil ecosystems. The abrupt hydrological disturbance differs from the nonstationarity in vegetation-climate interactions leading to chronic variable thresholds.

This study emphasizes the importance of stormflow thresholds as a diagnostic tool to effectively characterize abrupt variation in catchment emergent patterns and broad shift from slow to fast flood response, particularly with [temporal](#) nonstationarity in long-term interactions of abrupt earthquake-induced landslides and vegetation evolutions. The study

contributes to the mitigation and adaptive strategies for unpredictable hydrological regimes and flash flood disasters triggered by abrupt natural disturbances.

Data availability

405 The data that support the findings of this study are available from the corresponding author upon reasonable request.

Author Contributions

Guotao Zhang: Conceptualization, Methodology, Software, Data curation, Visualization. **Peng Cui:** Conceptualization, Supervision, Funding acquisition, Project administration. **Carlo Gualtieri:** Supervision, Writing – review & editing. **Nazir Ahmed Bazai:** Formal analysis, Writing – review & editing. **Xueqin Zhang:** Funding acquisition, Writing – review & editing.

410 **Zhengtao Zhang:** Software, investigation.

Competing interests

The authors declare that they have no known competing financial interests or personal relationships that could have appeared to influence the work reported in this paper.

Acknowledgments

415 This study was jointly supported by the National Natural Science Foundation of China (Grant No. U21A2008), the Second Tibetan Plateau Scientific Expedition and Research Program (STEP) (Grant No. 2019QZKK0903), [National Natural Science Foundation of China \(Grant No. 42201086\)](#), the National Postdoctoral Program for Innovative Talents (Grant No. BX20220293), the China Postdoctoral Science Foundation (Grant No. 2021M703180), and the Special Research Assistant program of the Chinese Academy of Sciences.

420 **References**

Ali, G., Oswald, C. J., Spence, C., Cammeraat, E. L. H., McGuire, K. J., Meixner, T., and Reaney, S. M.: Towards a unified threshold-based hydrological theory: necessary components and recurring challenges, *Hydrological Processes*, 27, 313-318, 10.1002/hyp.9560, 2013.

425 Ali, G., Tetzlaff, D., McDonnell, J. J., Soulsby, C., Carey, S., Laudon, H., McGuire, K., Buttle, J., Seibert, J., and Shanley, J.: Comparison of threshold hydrologic response across northern catchments, *Hydrological Processes*, 29, 3575-3591, 10.1002/hyp.10527, 2015.

- Arheimer, B. and Lindström, G.: Detecting changes in river flow caused by wildfires, storms, urbanization, regulation, and climate across Sweden, *Water Resources Research*, 55, 8990-9005, 10.1029/2019WR024759, 2019.
- 430 Bahmanpouri, F., Barbetta, S., Gualtieri, C., Ianniruberto, M., Filizola, N., Termini, D., and Moramarco, T.: Prediction of river discharges at confluences based on Entropy theory and surface-velocity measurements, *Journal of Hydrology*, 606, 127404, <https://doi.org/10.1016/j.jhydrol.2021.127404>, 2022.
- Beiter, D., Weiler, M., and Blume, T.: Characterising hillslope–stream connectivity with a joint event analysis of stream and groundwater levels, *Hydrology and Earth System Sciences*, 24, 5713-5744, 10.5194/hess-24-5713-2020, 2020.
- Beyen, K.: Hanging Wall and Footwall Effects in the Largest Reverse-Slip Earthquake of Turkey, October 23, 2011, $\mathbb{M}_{\mathbf{W}}7.2$ Van Earthquake, *Arabian Journal for Science and Engineering*, 44, 4757-4781, 10.1007/s13369-018-3547-x, 2019.
- 435 Bladon, K. D., Bywater-Reyes, S., LeBoldus, J. M., Kerio, S., Segura, C., Ritokova, G., and Shaw, D. C.: Increased streamflow in catchments affected by a forest disease epidemic, *Science of The Total Environment*, 691, 112-123, 10.1016/j.scitotenv.2019.07.127, 2019.
- 440 Bracken, L. J., Wainwright, J., Ali, G. A., Tetzlaff, D., Smith, M. W., Reaney, S. M., and Roy, A. G.: Concepts of hydrological connectivity: Research approaches, pathways and future agendas, *Earth-Science Reviews*, 119, 17-34, 10.1016/j.earscirev.2013.02.001, 2013.
- Brantley, S., Ford, C. R., and Vose, J. M.: Future species composition will affect forest water use after loss of eastern hem lock from southern Appalachian forests, *Ecological Applications*, 23, 777-790, <https://doi.org/10.1890/12-0616.1>, 2013.
- 445 Buttle, J. M., Webster, K. L., Hazlett, P. W., and Jeffries, D. S.: Quickflow response to forest harvesting and recovery in a northern hardwood forest landscape, *Hydrological Processes*, 33, 47-65, 10.1002/hyp.13310, 2019.
- Cain, M. R., Woo, D. K., Kumar, P., Keefer, L., and Ward, A. S.: Antecedent Conditions Control Thresholds of Tile-Runoff Generation and Nitrogen Export in Intensively Managed Landscapes, *Water Resources Research*, 58, 10.1029/2021wr030507, 2022.
- 450 Chen, Y. C.: Flood discharge measurement of mountain rivers, *Hydrology & Earth System Sciences Discussions*, 9, 12655-12690, 2012.
- Chiang, L.-C., Chuang, Y.-T., and Han, C.-C.: Integrating Landscape Metrics and Hydrologic Modeling to Assess the Impact of Natural Disturbances on Ecohydrological Processes in the Chenyulan Watershed, Taiwan, *International journal of environmental research and public health*, 16, 266, 10.3390/ijerph16020266, 2019.
- 455 Cui, P., Lin, Y., and Chen, C.: Destruction of vegetation due to geo-hazards and its environmental impacts in the Wenchuan earthquake areas, *Ecological Engineering*, 44, 61-69, 10.1016/j.ecoleng.2012.03.012, 2012.
- Deshmukh, D. S., Chaube, U. C., Ekube Hailu, A., Aberra Gudeta, D., and Tegene Kassa, M.: Estimation and comparison of curve numbers based on dynamic land use land cover change, observed rainfall-runoff data and land slope, *Journal of Hydrology*, 492, 89-101, 10.1016/j.jhydrol.2013.04.001, 2013.

设置了格式: 字体: 10 磅

设置了格式: 字体: 10 磅

设置了格式: 字体: 10 磅

设置了格式: 字体: 10 磅

- 460 Detty, J. M. and McGuire, K. J.: Threshold changes in storm runoff generation at a till-mantled headwater catchment, *Water Resources Research*, 46, 10.1029/2009wr008102, 2010.
- Dickinson, W. and Whiteley, H.: Watershed areas contributing to runoff, *IAHS publ*, 96, 12-26, 1970.
- Ebel, B. A.: Temporal evolution of measured and simulated infiltration following wildfire in the Colorado Front Range, USA: Shifting thresholds of runoff generation and hydrologic hazards, *Journal of Hydrology*, 124765, 2020.
- 465 Ebel, B. A. and Mirus, B. B.: Disturbance hydrology: challenges and opportunities, *Hydrological Processes*, 28, 5140-5148, 10.1002/hyp.10256, 2014.
- Eckhardt, K.: How to construct recursive digital filters for baseflow separation, *Hydrological Processes*, 19, 507-515, 10.1002/hyp.5675, 2005.
- Fan, X., Juang, C. H., Wasowski, J., Huang, R., Xu, Q., Scaringi, G., van Westen, C. J., and Havenith, H.-B.: What we have
470 learned from the 2008 Wenchuan Earthquake and its aftermath: A decade of research and challenges, *Engineering Geology*, 241, 25-32, 10.1016/j.enggeo.2018.05.004, 2018.
- Farrick, K. K. and Branfireun, B. A.: Soil water storage, rainfall and runoff relationships in a tropical dry forest catchment, *Water Resources Research*, 50, 9236-9250, 10.1002/2014WR016045, 2014.
- Farrick, K. K. and Branfireun, B. A.: Flowpaths, source water contributions and water residence times in a Mexican tropical
475 dry forest catchment, *Journal of Hydrology*, 529, 854-865, 10.1016/j.jhydrol.2015.08.059, 2015.
- Fu, C., Chen, J., Jiang, H., and Dong, L.: Threshold behavior in a fissured granitic catchment in southern China: 1. Analysis of field monitoring results, *Water Resources Research*, 49, 2519-2535, 10.1002/wrcr.20191, 2013a.
- Fu, C., Chen, J., Jiang, H., and Dong, L.: Threshold behavior in a fissured granitic catchment in southern China: 2. Modeling and uncertainty analysis, *Water Resources Research*, 49, 2536-2551, 10.1002/wrcr.20193, 2013b.
- 480 García-Gamero, V., Peña, A., Laguna, A. M., Giraldez, J. V., and Vanwallegem, T.: Factors controlling the asymmetry of soil moisture and vegetation dynamics in a hilly Mediterranean catchment, *Journal of Hydrology*, 598, 126207, <https://doi.org/10.1016/j.jhydrol.2021.126207>, 2021.
- Graham, C. B. and McDonnell, J. J.: Hillslope threshold response to rainfall: (2) Development and use of a macroscale model, *Journal of Hydrology*, 393, 77-93, 10.1016/j.jhydrol.2010.03.008, 2010.
- 485 Hahm, W. J., Rempe, D. M., Dralle, D. N., Dawson, T. E., Lovill, S. M., Bryk, A. B., Bish, D. L., Schieber, J., and Dietrich, W. E.: Lithologically Controlled Subsurface Critical Zone Thickness and Water Storage Capacity Determine Regional Plant Community Composition, *Water Resources Research*, 55, 3028-3055, 10.1029/2018wr023760, 2019.
- Hoek Van Dijke, A. J., Herold, M., Mallick, K., Benedict, I., Machwitz, M., Schlerf, M., Pranindita, A., Theeuwen, J. J. E., Bastin, J.-F., and Teuling, A. J.: Shifts in regional water availability due to global tree restoration, *Nature Geoscience*, 15, 363-
490 368, 10.1038/s41561-022-00935-0, 2022.
- Hong, N. M., Chu, H. J., Lin, Y. P., and Deng, D. P.: Effects of land cover changes induced by large physical disturbances on hydrological responses in Central Taiwan, *Environ Monit Assess*, 166, 503-520, 10.1007/s10661-009-1019-1, 2010.

设置了格式: 字体: 10 磅

设置了格式: 字体: 10 磅

- Huang, R. and Li, W.: Development and distribution of geohazards triggered by the 5.12 Wenchuan Earthquake in China, *Science in China Series E: Technological Sciences*, 52, 810-819, 10.1007/s11431-009-0117-1, 2009.
- 495 Hwang, T., Martin, K. L., Vose, J. M., Wear, D., Miles, B., Kim, Y., and Band, L. E.: Nonstationary Hydrologic Behavior in Forested Watersheds Is Mediated by Climate-Induced Changes in Growing Season Length and Subsequent Vegetation Growth, *Water Resources Research*, 54, 5359-5375, 10.1029/2017wr022279, 2018.
- John, A., Nathan, R., Horne, A., Fowler, K., and Stewardson, M.: Nonstationary Runoff Responses Can Interact With Climate Change to Increase Severe Outcomes for Freshwater Ecology, *Water Resources Research*, 58, 10.1029/2021wr030192, 2022.
- 500 Kirchner, J. W.: Catchments as simple dynamical systems: Catchment characterization, rainfall-runoff modeling, and doing hydrology backward, *Water Resources Research*, 45, 10.1029/2008wr006912, 2009.
- Knowles, J. F., Lestak, L. R., and Molotch, N. P.: On the use of a snow aridity index to predict remotely sensed forest productivity in the presence of bark beetle disturbance, *Water Resources Research*, 53, 4891-4906, <https://doi.org/10.1002/2016WR019887>, 2017.
- 505 Maina, F. Z. and Siirila-Woodburn, E. R.: Watersheds dynamics following wildfires: Nonlinear feedbacks and implications on hydrologic responses, *Hydrological Processes*, 34, 33-50, 10.1002/hyp.13568, 2019.
- Major, J. J. and Mark, L. E.: Peak flow responses to landscape disturbances caused by the cataclysmic 1980 eruption of Mount St. Helens, Washington, *Geological Society of America Bulletin*, 118, 938-958, 2006.
- McDonnell, J. J., Spence, C., Karran, D. J., Ilja van Meerveld, H. J., and Harman, C.: Fill-and-spill: A process description of runoff generation at the scale of the beholder, *Water Resources Research*, 57, e2020WR027514, 10.1029/2020WR027514, 2021.
- 510 Menberu, M. W., Tahvanainen, T., Marttila, H., Irannezhad, M., Ronkanen, A.-K., Penttinen, J., and Kløve, B.: Water-table-dependent hydrological changes following peatland forestry drainage and restoration: Analysis of restoration success, *Water Resources Research*, 52, 3742-3760, <https://doi.org/10.1002/2015WR018578>, 2016.
- 515 Mirus, B. B., Smith, J. B., and Baum, R. L.: Hydrologic Impacts of Landslide Disturbances: Implications for Remobilization and Hazard Persistence, *Water Resources Research*, 53, 8250-8265, 10.1002/2017wr020842, 2017a.
- Mirus, B. B., Ebel, B. A., Mohr, C. H., and Zegre, N.: Disturbance hydrology: Preparing for an increasingly disturbed future, *Water Resources Research*, 53, 10007-10016, 2017b.
- 520 Montgomery, D. R. and Manga, M.: Streamflow and water well responses to earthquakes, *Science*, 300, 2047-2049, 10.1126/science.1082980, 2003.
- Moody, J. A., Shakesby, R. A., Robichaud, P. R., Cannon, S. H., and Martin, D. A.: Current research issues related to post-wildfire runoff and erosion processes, *Earth-Science Reviews*, 122, 10-37, 10.1016/j.earscirev.2013.03.004, 2013.
- Moramarco, T., Saltalippi, C., and Singh, V. P.: Estimation of Mean Velocity in Natural Channels Based on Chiu's Velocity Distribution Equation, *Journal of Hydrologic Engineering*, 9, 42-50, 2004.

设置了格式: 字体: 10 磅

设置了格式: 字体: 10 磅

设置了格式: 字体: 10 磅

设置了格式: 字体: 10 磅

- 525 Moreno-de-las-Heras, M., Merino-Martín, L., Saco, P. M., Espigares, T., Gallart, F., and Nicolau, J. M.: Structural and functional control of surface-patch to hillslope-scale runoff and sediment connectivity in Mediterranean-dry reclaimed slope systems, *Hydrology and Earth System Sciences Discussions*, 1-28, 2020.
- Muggeo, V. M. R.: Estimating regression models with unknown break-points, *Statistics in Medicine*, 22, 3055-3071, 10.1002/sim.1545, 2003.
- 530 Murphy, S. F., McCleskey, R. B., Martin, D. A., Writer, J. H., and Ebel, B. A.: Fire, Flood, and Drought: Extreme Climate Events Alter Flow Paths and Stream Chemistry, *Journal of Geophysical Research: Biogeosciences*, 123, 2513-2526, <https://doi.org/10.1029/2017JG004349>, 2018.
- Oswald, C. J., Richardson, M. C., and Branfireun, B. A.: Water storage dynamics and runoff response of a boreal Shield headwater catchment, *Hydrological Processes*, 25, 3042-3060, 10.1002/hyp.8036, 2011.
- 535 Penna, D., Tromp-van Meerveld, H., Gobbi, A., Borga, M., and Dalla Fontana, G.: The influence of soil moisture on threshold runoff generation processes in an alpine headwater catchment, *Hydrology and Earth System Sciences*, 15, 689-702, 10.5194/hess-15-689-2011, 2011.
- Pierson, T. C., Major, J. J., Amigo, Á., and Moreno, H.: Acute sedimentation response to rainfall following the explosive phase of the 2008–2009 eruption of Chaitén volcano, Chile, *Bulletin of Volcanology*, 75, 723, 10.1007/s00445-013-0723-4, 2013.
- 540 Ran, Q., Qian, Q., Li, W., Fang, Q., Fu, X., Yu, X., and Yueping, X.: Impact of earthquake-induced-landslides on hydrologic response of a steep mountainous catchment: a case study of the Wenchuan earthquake zone, *Journal of Zhejiang University SCIENCE A*, 16, 131-142, 10.1631/jzus.A1400039, 2015.
- Ross, C. A.: Moving towards a unified threshold-based hydrological theory through inter-comparison and modelling, 2021.
- Ross, C. A., Ali, G. A., Spence, C., and Courchesne, F.: Evaluating the Ubiquity of Thresholds in Rainfall-Runoff Response Across Contrasting Environments, *Water Resources Research*, 57, 10.1029/2020wr027498, 2021.
- 545 Scaife, C. I. and Band, L. E.: Nonstationarity in threshold response of stormflow in southern Appalachian headwater catchments, *Water Resources Research*, 53, 6579-6596, 10.1002/2017wr020376, 2017.
- Scaife, C. I., Singh, N. K., Emanuel, R. E., Miniati, C. F., and Band, L. E.: Non-linear quickflow response as indicators of runoff generation mechanisms, *Hydrological Processes*, 34, 2949-2964, 10.1002/hyp.13780, 2020.
- 550 Seidl, R., Thom, D., Kautz, M., Martin-Benito, D., Peltoniemi, M., Vacchiano, G., Wild, J., Ascoli, D., Petr, M., Honkaniemi, J., Lexer, M. J., Trotsiuk, V., Mairota, P., Svoboda, M., Fabrika, M., Nagel, T. A., and Reyser, C. P. O.: Forest disturbances under climate change, *Nature Climate Change*, 7, 395-402, 10.1038/nclimate3303, 2017.
- Shafique, M.: Spatial and temporal evolution of co-seismic landslides after the 2005 Kashmir earthquake, *Geomorphology*, 362, 107228, 10.1016/j.geomorph.2020.107228, 2020.
- 555 Shangguan, W., Hengl, T., Mendes De Jesus, J., Yuan, H., and Dai, Y.: Mapping the global depth to bedrock for land surface modeling, *Journal of Advances in Modeling Earth Systems*, 9, 65-88, 10.1002/2016ms000686, 2017.
- Shen, P., Zhang, L. M., Fan, R. L., Zhu, H., and Zhang, S.: Declining geohazard activity with vegetation recovery during first ten years after the 2008 Wenchuan earthquake, *Geomorphology*, 352, 106989, 10.1016/j.geomorph.2019.106989, 2020.

设置了格式: 字体: 10 磅

设置了格式: 字体: 10 磅

- 560 Shuttleworth, E. L., Evans, M. G., Pilkington, M., Spencer, T., Walker, J., Milledge, D., and Allott, T. E. H.: Restoration of blanket peat moorland delays stormflow from hillslopes and reduces peak discharge, *Journal of Hydrology* X, 2, 100006, <https://doi.org/10.1016/j.hydroa.2018.100006>, 2019.
- 565 Sidle, R. C., Gomi, T., Loaiza Usuga, J. C., and Jarihani, B.: Hydrogeomorphic processes and scaling issues in the continuum from soil pedons to catchments, *Earth-Science Reviews*, 175, 75-96, 10.1016/j.earscirev.2017.10.010, 2017.
- Tromp-van Meerveld, H. J. and McDonnell, J. J.: Threshold relations in subsurface stormflow: 1. A 147-storm analysis of the Panola hillslope, *Water Resources Research*, 42, 336-336, 10.1029/2004WR003778, 2006.
- Tunas, I. G., Tanga, A., and Oktavia, S.: Impact of Landslides Induced by the 2018 Palu Earthquake on Flash Flood in Bangga River Basin, Sulawesi, Indonesia, *Journal of Ecological Engineering*, 21, 190-200, 10.12911/22998993/116325, 2020.
- 570 Wang, J., Jin, W., Cui, Y.-f., Zhang, W.-f., Wu, C.-h., and Alessandro, P.: Earthquake-triggered landslides affecting a UNESCO Natural Site: the 2017 Jiuzhaigou Earthquake in the World National Park, China, *Journal of Mountain Science*, 15, 1412-1428, 10.1007/s11629-018-4823-7, 2019.
- Wang, S., Yan, Y., Fu, Z., and Chen, H.: Rainfall-runoff characteristics and their threshold behaviors on a karst hillslope in a peak-cluster depression region, *Journal of Hydrology*, 605, 10.1016/j.jhydrol.2021.127370, 2022.
- Wei, L., Qiu, Z., Zhou, G., Kinouchi, T., and Liu, Y.: Stormflow threshold behaviour in a subtropical mountainous headwater catchment during forest recovery period, *Hydrological Processes*, 34, 1728-1740, 10.1002/hyp.13658, 2020.
- 575 Xu, C., Xu, X., Yao, X., and Dai, F.: Three (nearly) complete inventories of landslides triggered by the May 12, 2008 Wenchuan Mw 7.9 earthquake of China and their spatial distribution statistical analysis, *Landslides*, 11, 441-461, 10.1007/s10346-013-0404-6, 2013.
- Xu, Q., Zhang, S., and Li, W.: Spatial distribution of large-scale landslides induced by the 5.12 Wenchuan Earthquake, *Journal of Mountain Science*, 8, 246-260, 10.1007/s11629-011-2105-8, 2011.
- 580 Yunus, A. P., Fan, X., Tang, X., Jie, D., Xu, Q., and Huang, R.: Decadal vegetation succession from MODIS reveals the spatio-temporal evolution of post-seismic landsliding after the 2008 Wenchuan earthquake, *Remote Sensing of Environment*, 236, 111476, 10.1016/j.rse.2019.111476, 2020.
- Zehe, E. and Sivapalan, M.: Threshold behaviour in hydrological systems as (human) geo-ecosystems: manifestations, controls, implications, *Hydrology and Earth System Sciences*, 13, 1273-1297, 10.5194/hess-13-1273-2009, 2009.
- 585 Zehe, E., Elsenbeer, H., Lindenmaier, F., Schulz, K., and Blöschl, G.: Patterns of predictability in hydrological threshold systems, *Water Resources Research*, 43, 10.1029/2006wr005589, 2007.
- Zhang, G., Cui, P., Jin, W., Zhang, Z., Wang, H., Bazai, N. A., Li, Y., Liu, D., and Pasuto, A.: Changes in hydrological behaviours triggered by earthquake disturbance in a mountainous watershed, *Science of The Total Environment*, 760, 143349, 10.1016/j.scitotenv.2020.143349, 2021a.
- 590 Zhang, G., Cui, P., Gualtieri, C., Zhang, J., Ahmed Bazai, N., Zhang, Z., Wang, J., Tang, J., Chen, R., and Lei, M.: Stormflow generation in a humid forest watershed controlled by antecedent wetness and rainfall amounts, *Journal of Hydrology*, 603, 127107, <https://doi.org/10.1016/j.jhydrol.2021.127107>, 2021b.

设置了格式: 字体: 10 磅

设置了格式: 字体: 10 磅

设置了格式: 字体: 10 磅

设置了格式: 字体: 10 磅

Zhang, J., van Meerveld, H. J., Tripoli, R., and Bruijnzeel, L. A.: Runoff response and sediment yield of a landslide-affected fire-climax grassland micro-catchment (Leyte, the Philippines) before and after passage of typhoon Haiyan, *Journal of Hydrology*, 565, 524-537, 10.1016/j.jhydrol.2018.08.016, 2018.

